

Wideband versatile radio-frequency spectrum analyzer

V. Lavielle, I. Lorgeré, and J.-L. Le Gouët

Laboratoire Aimé Cotton, Centre National de la Recherche Scientifique, Bâtiment 505, 91405 Orsay Cédex, France

S. Tonda and D. Dolfi

Thales TRT, Domaine de Corbeville, 91404 Orsay Cédex, France

Received September 24, 2002

Operation of a wideband, versatile optical spectrum analyzer for radio-frequency (RF) signals is demonstrated. The device is based on spectral hole burning (SHB). The demonstration features 2.3-GHz instantaneous bandwidth, 500-kHz resolution, and a 32-dB dynamic range. A true RF signal, transferred to the optical carrier with the help of a Mach-Zehnder modulator, is analyzed with optical carrier suppression and zooming capabilities. This is to the authors' knowledge the largest instantaneous bandwidth ever demonstrated for a SHB-based processor in rare-earth-doped crystals. © 2003 Optical Society of America

OCIS codes: 070.4790, 300.6370, 350.1260, 190.4380, 090.4220, 070.4340.

Astronomers are expecting valuable information from the submillimeter window, frequencies from 300 GHz to 3 THz, where numerous important molecular and atomic species have unique spectral fingerprints. Heterodyne detection is employed for submillimeter signals. One mixes the astronomical signal with a stable local oscillator to translate the signal to a much lower frequency, in the 1–10-GHz range. Amplifiers and high-resolution spectrometers are available in this frequency range. Cryogenic conditions are necessary for both high-frequency mixers and low-noise amplifiers.

Also, one needs broadband spectrometers at the back end of heterodyne detection chains. Available spectrometers do not satisfy the bandwidth demand. The forthcoming Herschel Space Observatory will use four acousto-optical spectrometers (AOSs) to cover an instantaneous bandwidth of 4 GHz with a resolution of 1 MHz. Inasmuch as the AOSs have fixed resolution and bandwidth, an autocorrelation spectrometer with a maximum resolution of 100 kHz will also be used. The ACS is flexible but still suffers from limited bandwidth, below 500 MHz, and high power consumption. If such combinations of spectrometers can handle a 4-GHz bandwidth, they cannot cope with increasing bandwidth demand. Alternative technology will be required for future space laboratories.

The emerging spectral hole burning (SHB) technology has the potential to treat this large bandwidth. Specifically, the inhomogeneously broadened absorption bands of rare-earth-doped crystals have bandwidths that exceed 10 GHz, 100 GHz in some cases, together with spectral resolution well below 100 kHz at low temperature. Spatial-spectral coherent filters can be engraved in these materials, permitting numerous optical signal processing operations pioneered by Mossberg's research on optical memories.¹ With the advent of broadband integrated electro-optic modulators, these materials are particularly suited to processing broadband radio-frequency (RF) signals with impressive time-bandwidth products. True time delay for phased array antennas,²

correlators,³ Fourier transformers,⁴ and laser stabilization⁵ are among the applications that are being pursued. The principle of a spectral analyzer for broadband RF signals based on SHB was recently proposed and demonstrated.⁶ In this Letter we demonstrate broadband operation of such a device. This is what is to our knowledge the first SHB-based processor to demonstrate an instantaneous bandwidth above 1 GHz. As an optical spectrum analyzer for RF signals, this device has a larger bandwidth than and resolution and dynamic range similar to those of available AOS. In addition, unique important features such as multiscale spectral analysis and optical carrier suppression are reported for what we believe is the first time.

The spectral analyzer operates as follows: One first engraves a holographic filter in the absorption band of the crystal. The two engraving beams issue from the same laser. During this engraving stage of duration τ , the frequency of the laser is linearly swept over a frequency interval $\Delta\nu$ while the angle between the two beams is simultaneously linearly scanned over an angular range $\Delta\theta$. Because of the intrinsic frequency selectivity of the SHB process in the crystal, a specific diffraction direction is thus assigned to each frequency component. If a monochromatic laser beam modulated by a RF signal reads this holographic filter, the spectral components of the RF signal are then angularly resolved. The dispersion law is given by the coefficient $\Delta\theta/\Delta\nu$ or, equivalently, by the ratio θ/r , where r is the laser chirp rate and θ is the angular scan rate. The spectral resolution is ultimately limited by the homogeneous linewidth of the ion transition, and the bandwidth is limited by the inhomogeneous width. The maximum number of channels is therefore ultimately limited by the time-bandwidth product of the crystal. However, the number of resolvable channels is diffraction limited. The angular FWHM of a channel is $\delta\theta = 0.46\lambda/w$, where w is the Gaussian beam waist on the crystal. The number of channels is $\Delta\theta/\delta\theta$, which is also the ratio $\Delta\nu/\delta\nu$, where $\delta\nu$ is the spectral resolution.

For given beam waist and angular range, as in the experiments reported below, the number of channels is fixed. Reducing the bandwidth thus increases spectral resolution.

The experiments are performed with the 793-nm absorption line of a 2.5-mm-long 0.5-at.% doped Tm^{3+} :YAG crystal maintained at 5 K by a helium flow. The inhomogeneous absorption line is ~ 20 GHz wide, with a homogeneous linewidth of ~ 150 kHz. The frequency agile laser is an external-cavity diode laser tuned by an electro-optic wedge.⁷ It performs 50-GHz mode-hop-free sweeping range with a precision and stability of 500 kHz on a 10-ms time scale. Engraving beams 1 and 2 are split from the laser output beam. Beam 1 goes through a pair of acousto-optic deflectors whose deflection angles are added while the associated frequency shifts are subtracted. The two ~ 5 -mW beams cross on the same 220- μm FWHM spot in the crystal, which is set in an imaging position with respect to the acousto-optic deflectors such that beam 1's position on the crystal remains fixed during angular scans. The holographic filter is recorded in the 3H_6 - 3H_4 transition of Tm^{3+} ions. The engraved filter's lifetime is ~ 10 ms. Consequently, it must be continually refreshed. The engraving periods, each 250 μs long, are therefore repeated at a 2-kHz rate. This accumulated engraving procedure ensures quasi-stationary diffraction efficiency and decreases the necessary engraving power. The box geometry described previously⁶ achieves angular separation of all the beams on the crystal and therefore permits simultaneous hologram engraving, reading by the probe beam, and diffracted signal collection. In the present setup the probe beam that is carrying the RF signal is split from the same laser beam as are the engraving beams. Consequently, spectral analysis can be performed only in the 250- μs -long intervals between successive engraving periods. The experiments consist of repetition of these engrave-analyze cycles. Under these conditions, one achieves a 50% probability of intercept for the analyzer. Two independent lasers are necessary for reaching a 100% probability of intercept, which is the objective of some forthcoming experiments. The signal is detected by a 1024-element photodiode array (PDA) in the focal plane of a converging lens. The array reading is not synchronized with the engrave-analyze cycles. Simple spatial filtering of the signal beam eliminates most stray light from the powerful engraving beams.⁶

In a first experiment, the laser frequency is linearly swept over the interval $[\nu_0; \nu_0 + \Delta\nu]$ during the engraving period and then goes back to the value $\nu_0 + \Delta\nu/2$, where it stays for the whole analysis period until the next engraving period. A 5- μs -long pulse is crafted in the 1.2-mW probe beam in the analysis phase. One thus simulates a single radio frequency. Curve (a) of Fig. 1 shows a sample record of the PDA signal. For these data the laser sweep range is set at 1 GHz. The angular scanning range is 86 mrad, as it is for all experiments reported here. The angular FWHM of the detected line is 2.8 mrad, which is the expected value. Consequently, the number of frequency

channels is 30 for all experiments reported here. One notices the very low background, essentially given by residual stray light from the probe beam. The high signal level is obtained as a result of the accumulation procedure. The simple fact that the accumulation indeed works is a breakthrough in itself. We believe that this is the first time that the accumulated engraving of a broadband SHB processor has been demonstrated with a frequency agile laser, thus opening the way to SHB processors with bandwidths by far exceeding that of the electronics.

We use the same single-frequency reading experiment to study the dynamic range of the spectrometer. The probe power can be varied over the whole 32-dB dynamic range of the PDA. The minimum average probe power that will give rise to a detectable signal on the PDA noise floor is only 30 nW. Another important feature that we observe is the absence of angular line broadening for large probe power, as illustrated in curve (b) of Fig. 1, which shows curve (a), a strong line, on a logarithmic scale. The wings of the line fall to background level within less than 10 mrad. Hence a faint spectral line can be detected in the wings of a strong line. The nonzero background is actually due to stray light from the probe beam. This light can be eliminated. Also, careful spatial filtering of the beams impinging on the crystal will reduce the extent of the line wing.

In a second experiment, after the interval $[\nu_0; \nu_0 + \Delta\nu]$ is engraved the laser frequency goes back to ν_0 and then climbs 19 even stairs that span the whole $\Delta\nu$ interval. Each step is 5 μs long. One thus simulates a comb RF spectrum. Curve (c) of Fig. 1 shows a sample of the detected signal. In this experiment the analyzer bandwidth $\Delta\nu$ is set at 2.3 GHz, which is to our knowledge the largest instantaneous bandwidth ever demonstrated for a SHB-based processor. It also is larger than current AOS bandwidths. The FWHM of the detected lines is not affected by the number of lines. Neither is the diffraction efficiency of each individual line. It is only the breakdown of our antireflection-coated diode that prevented us from experimenting with larger bandwidths.

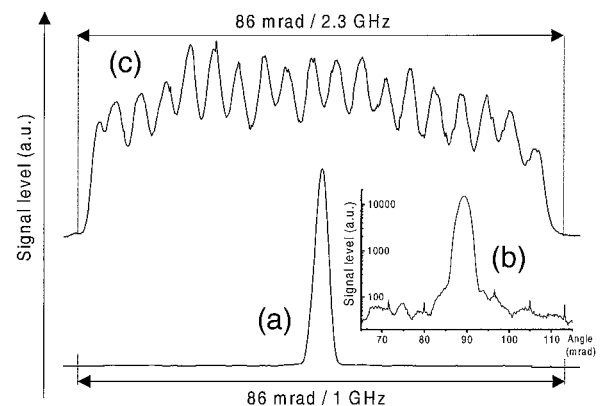


Fig. 1. Detected signal in a PDA for (a) an analyzer bandwidth of 1 GHz and a single RF reading and (c) an analyzer bandwidth of 2.3 GHz and a 19-line comb RF spectrum. In both cases the angular range is 86 mrad. (b) Same record as in (a) but on a logarithmic vertical scale.

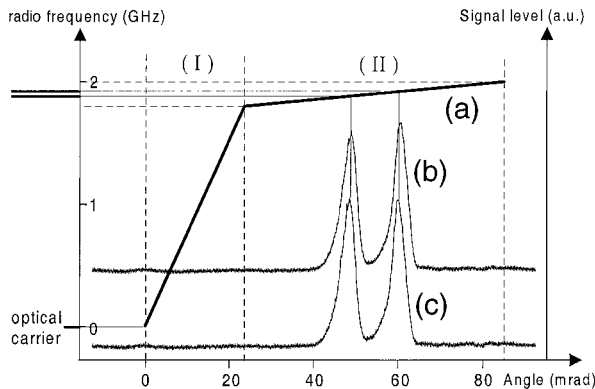


Fig. 2. Multiscale spectral analysis of a RF signal. (a) The $\theta = f(\nu)$ transfer function of the spectral analyzer. The spectrum of the probe beam, carrying a 1.85-GHz RF sine wave that is square-frequency modulated at 40 MHz, is shown on the RF axis. Experimental records show the corresponding detected signal as (c) given by a single reading of the PDA or (b) averaged over 100 PDA readings. The signal in area (I) of the PDA window is a low-resolution projection ($\theta/r_1 = 13.4$ mrad/GHz) of the (0–1.8-GHz) RF interval. A slower frequency scan ($\theta/r_2 = 310$ mrad/GHz) in window (II) zooms on the region of interest.

Next we demonstrate spectral analysis of a true RF signal. The RF signal is transferred to the probe beam with the help of a Mach–Zehnder electro-optic modulator. In most applications this RF modulation is made near the half-wave voltage of the modulator. The modulated light-field spectrum then contains the optical carrier line and the two symmetric sidebands of the RF signal. However, for purposes of spectral analysis, only one RF sideband is necessary, and no optical carrier. Fortunately our spectrometer can analyze a single RF sideband without the need for an optical carrier. Consequently the modulator can be operated in the zero-point modulation configuration, which suppresses the optical carrier. No probe power reaches the spectrometer in the absence of RF modulation, a condition that contributes to a high signal-to-noise ratio. The laser frequency for probing can be set such that only a single sideband passes through the spectrometer.

In this experiment the laser frequency is swept at rate r_1 during the first 28% of the engraving period and at a rate $r_2 \ll r_1$ during the remaining 72% of the engraving time. The angular scan rate is constant during the whole engraving period. Consequently the $\theta = f(\nu)$ projection function of the spectrum analyzer is a two-slope function, as shown in curve (a) of Fig. 2. The first part of the analyzer bandwidth, which covers 90% of analyzer bandwidth $\Delta\nu$, is projected over only 28% of the angular range. The dispersion coefficient is low and the spectral resolution poor. The last 10% of the analyzer bandwidth is spread over 72% of the angular range. Dispersion is high. So is spectral resolution. The ratio of the spectral resolution in the two spectral bands is 23. In this way one can analyze at high resolution a highly pitched RF spectrum while still achieving wide spectral cov-

erage. This fact is of practical relevance in radar applications and also in astronomy, for which the large bandwidth is actually composed of several bands and different resolutions are required. It is noteworthy that the transfer function of the analyzer can be dynamically adapted to the input RF signal. The adaptation time is limited by the ~ 10 -ms hologram lifetime. For the records shown in Fig. 2 the bandwidth of the analyzer is set at 2 GHz. The RF signal fed to the modulator is a 1.85-GHz sine wave, square-frequency modulated at 40 MHz. The bias voltage on the modulator is set to minimize the optical carrier. The two-tone spectrum of the RF signal falls into the high-resolution part of the analyzer bandwidth and thus can be resolved. One can identify the faint remaining optical carrier line, which is at the frequency of the start of the analyzer bandwidth, in the low-resolution region.

The high resolution is 9 MHz in this experiment. The ultimate resolution that we can achieve with the present setup is 500 kHz, limited by the laser linewidth. Another important point for astronomy is the possibility of integration of the RF spectrum for a long time. The spectrum must be stable on the PDA. Curve (b) of Fig. 2 shows an average over 100 readings of the PDA, which represents an integration over 1 s. Curve (c) shows a sample of these 100 readings. The angular width of the average is the same as that of a single shot, which demonstrates capability for long integration times.

In conclusion, we have demonstrated wideband operation of a SHB-based spectrum analyzer for RF signals. The setup reported here surpasses current AOS technology in bandwidth and features similar a dynamic range and resolution. In contrast with AOSs, it is flexible in bandwidth and resolution, is optical carrier free, and has the potential for bandwidths exceeding 10 GHz. Increasing the bandwidth, the number of channels, and the probability of intercept are objectives of our planned experiments.

We are very grateful to the European Space Agency for continuing support (contracts ESA 12876/98/NL/MV and ESTEC 14174/00/NL/SB). Discussions with L. Pagani were very enriching and encouraging. The assistance of Salah Boussen in the RF experiments was invaluable. V. Lavielle's e-mail address is vincent.lavielle@lac.u-psud.fr.

References

1. T. W. Mossberg, *Opt. Lett.* **27**, 77 (1982).
2. K. D. Merkel, W. R. Babbitt, K. E. Anderson, and K. H. Wagner, *Opt. Lett.* **24**, 1386 (1999).
3. T. L. Harris, Y. Sun, W. R. Babbitt, R. L. Cone, J. A. Ritcey, and R. W. Equall, *Opt. Lett.* **25**, 85 (2000).
4. L. Ménager, J.-L. Le Gouët, and I. Lorgeré, *Opt. Lett.* **26**, 1397 (2001).
5. T. Böttger, Y. Sun, G. J. Pryde, G. Reinemer, and R. L. Cone, *J. Lumin.* **94–95**, 565 (2001).
6. L. Ménager, I. Lorgeré, J.-L. Le Gouët, D. Dolfi, and J.-P. Huignard, *Opt. Lett.* **26**, 1245 (2001).
7. L. Levin, *Opt. Lett.* **27**, 237 (2002).